EUROPEAN ORGANIZATION FOR NUCLEAR RESEARCH (CERN)

CERN-EP-2021-092
LHCb-PAPER-2021-014
October 6, 2021

Branching fraction measurements of the rare $B_s^0 \to \phi\mu^+\mu^-$ and $B_s^0 \to f_2'(1525)\mu^+\mu^-$ decays

LHCb collaboration[†]

Abstract

The branching fraction of the rare $B_s^0 \to \phi\mu^+\mu^-$ decay is measured using data collected by the LHCb experiment at center-of-mass energies of 7, 8 and 13 TeV, corresponding to integrated luminosities of 1, 2 and 6 fb^{-1}, respectively. The branching fraction is reported in intervals of q^2, the square of the dimuon invariant mass. In the q^2 region between 1.1 and 6.0 GeV^2/c^4, the measurement is found to lie 3.6 standard deviations below a Standard Model prediction based on a combination of Light Cone Sum Rule and Lattice QCD calculations. In addition, the first observation of the rare $B_s^0 \to f_2'(1525)\mu^+\mu^-$ decay is reported with a statistical significance of nine standard deviations and its branching fraction is determined.

Published in Phys. Rev. Lett. **127** (2021) 151801

[†]Authors are listed at the end of this paper.

Recent studies of rare semileptonic $b \to s\ell^+\ell^-$ decays exhibit tensions between experimental results and Standard Model (SM) predictions of branching fractions [1–5], angular distributions [6–11], and lepton universality [11–19]. Since these decays are only allowed via higher-order electroweak (loop) diagrams in the SM, they constitute powerful probes for non-SM contributions. One of the most significant discrepancies appears in the branching fraction of the $B^0_s \to \phi\mu^+\mu^-$ decay [1,2]. Using $3\,\text{fb}^{-1}$ of data collected with the LHCb experiment at center-of-mass energies of 7 and 8 TeV, the branching fraction was measured below the SM prediction at the level of three standard deviations (σ) [1]. This Letter presents an updated measurement using data taken at center-of-mass energies of 7, 8 and 13 TeV during the 2011, 2012 and 2015–2018 data-taking periods, with integrated luminosities corresponding to 1, 2 and $6\,\text{fb}^{-1}$, respectively. Compared to the $3\,\text{fb}^{-1}$ sample alone, this represents an increase of about a factor of four in the number of produced B^0_s mesons. The branching fraction is determined in intervals of q^2, the squared invariant mass of the dimuon system. In addition, the observation of the $B^0_s \to f'_2(1525)\mu^+\mu^-$ decay and a determination of its branching fraction are reported. This constitutes the first observation of a rare semileptonic decay involving a spin-2 meson in the final state, and provides complementary information to transitions involving pseudoscalar or vector mesons. In the following, the shorthand notation f'_2 is used to refer to the $f'_2(1525)$ meson. The inclusion of charge-conjugate processes is implied throughout.

The LHCb detector is a single-arm forward spectrometer covering the pseudorapidity range $2 < \eta < 5$, detailed in Refs. [20, 21]. The online event selection is performed by a trigger [22] that consists of hardware and software stages. The former selects signal candidates containing a muon with significant transverse momentum with respect to the beam axis. At the software stage, a full event reconstruction is applied. Simulated events are used in this analysis to determine the reconstruction and selection efficiency of signal candidates, and to estimate contamination from residual background. The simulated samples are produced using the software described in Refs. [23–25]. Residual mismodeling in simulation is corrected for using control samples from data.

The $B^0_s \to \phi\mu^+\mu^-$ and $B^0_s \to f'_2\mu^+\mu^-$ decays are reconstructed in the $K^+K^-\mu^+\mu^-$ final state. Particle identification criteria are applied to the kaon and muon candidates. The muons (kaons) are further required to have $\chi^2_{\text{IP}} > 9(6)$ with respect to any primary pp interaction vertex (PV) in the event, where χ^2_{IP} denotes the difference in the vertex-fit χ^2 of the PV when reconstructed with or without the considered track. The four final-state tracks are fit to a common vertex that is required to have good quality and to be significantly displaced from any PV in the event. Signal candidates are retained if the $K^+K^-\mu^+\mu^-$ invariant mass, $m(K^+K^-\mu^+\mu^-)$, lies between 5270 and 5700 MeV/c^2. The invariant mass of the dikaon system, $m(K^+K^-)$, is required to be within $12\,\text{MeV}/c^2$ of the known ϕ mass for the $B^0_s \to \phi\mu^+\mu^-$ decay, or within $225\,\text{MeV}/c^2$ of the known mass of the wider f'_2 resonance for the $B^0_s \to f'_2\mu^+\mu^-$ decay [26].

The q^2 regions between 8.0 and $11.0\,\text{GeV}^2/c^4$, and between 12.5 and $15.0\,\text{GeV}^2/c^4$, are dominated by tree-level B^0_s decays into final states with a J/ψ or $\psi(2S)$ meson. While these regions are vetoed in the selection of the signal modes, the decays to charmonium are used as high-yield control modes. The $B^0_s \to J/\psi\phi$ decay is used for normalization. The q^2 region from 0.98 to $1.1\,\text{GeV}^2/c^4$ is also vetoed to remove contributions from $B^0_s \to \phi(\to \mu^+\mu^-)\phi$ decays.

To reduce combinatorial background, formed from random track combinations, a boosted decision tree (BDT) algorithm [27, 28] is applied. The BDT classifier is trained

on data using cross-validation techniques [29], with $B_s^0 \to J/\psi\phi$ events as signal proxy and candidates from the upper mass sideband $m(K^+K^-\mu^+\mu^-) > 5567\,\text{MeV}/c^2$ as background proxy. The classifier combines the B_s^0 transverse momentum and χ^2_{IP}, the angle between the B_s^0 momentum and the vector connecting the PV and the decay vertex of the B_s^0 candidate, the fit quality of the B_s^0 vertex and its displacement from the associated PV, particle identification information and χ^2_{IP} of the final-state particles.

The criterion on the BDT output is optimized by maximizing the expected significance of the $B_s^0 \to \phi\mu^+\mu^-$ and $B_s^0 \to f_2'\mu^+\mu^-$ signals separately, due to different levels of background contamination. The requirement on the BDT classifier yields a signal efficiency of 96% (85%) and a background rejection of 96% (95%) for the $B_s^0 \to \phi\mu^+\mu^-$ ($B_s^0 \to f_2'\mu^+\mu^-$) decay mode. Finally, information from particle identification is combined with invariant mass variables, constructed under the relevant particle-hypotheses, to reject background from $\Lambda_b^0 \to pK^-\mu^+\mu^-$ decays, where the proton is misidentified as a kaon, and from $B_s^0 \to J/\psi\phi$, $B_s^0 \to \psi(2S)\phi$ and $B^0 \to J/\psi K^{*0}$ decays, where a final state hadron is misreconstructed as a muon and vice-versa.

The differential branching fraction of the $B_s^0 \to \phi\mu^+\mu^-$ decay is determined in intervals of q^2, relative to the $B_s^0 \to J/\psi\phi$ normalization mode, according to

$$\frac{\mathrm{d}\mathcal{B}(B_s^0 \to \phi\mu^+\mu^-)}{\mathrm{d}q^2} = \frac{\mathcal{B}(B_s^0 \to J/\psi\phi) \times \mathcal{B}(J/\psi \to \mu^+\mu^-)}{q^2_{\text{max}} - q^2_{\text{min}}} \times \frac{N_{\phi\mu^+\mu^-}}{N_{J/\psi\phi}} \times \frac{\epsilon_{J/\psi\phi}}{\epsilon_{\phi\mu^+\mu^-}}, \quad (1)$$

where $N_{J/\psi\phi}$ and $\epsilon_{J/\psi\phi}$ are the yields and efficiencies of the normalization mode, and $N_{\phi\mu^+\mu^-}$ and $\epsilon_{\phi\mu^+\mu^-}$ the corresponding parameters for the signal mode in the $[q^2_{\text{min}}, q^2_{\text{max}}]$ interval. The branching fractions related to the normalization mode are given by $\mathcal{B}(B_s^0 \to J/\psi\phi) = (1.018 \pm 0.032 \pm 0.037) \times 10^{-3}$ [30] and $\mathcal{B}(J/\psi \to \mu^+\mu^-) = (5.961 \pm 0.033)\,\%$ [26].

As the relative efficiencies vary according to the data-taking conditions, the data are split into the 2011–2012, 2015–2016 and 2017–2018 periods. The yields of the normalization mode for the different data-taking periods are determined using extended unbinned maximum-likelihood fits to the $m(K^+K^-\mu^+\mu^-)$ distribution. The $B_s^0 \to J/\psi\phi$ decay is modeled using the sum of two Gaussian functions with a common mean and a power-law tail towards upper and lower mass. The combinatorial background is modeled using an exponential function. The $m(K^+K^-\mu^+\mu^-)$ distribution of the normalization mode for the full data sample, overlaid with the fit projections, is shown in Fig. 1 (left). The yields of the normalization mode, $N_{J/\psi\phi}$, are determined to be $62\,980 \pm 270$, $70\,970 \pm 290$, and $148\,490 \pm 410$ for the three different data-taking periods, where the uncertainties are statistical only.

For the rare $B_s^0 \to \phi\mu^+\mu^-$ decay, a simultaneous extended maximum-likelihood fit of the data samples for the different periods is performed in intervals of q^2, where the signal yields are parameterized using Eq. (1) and the differential branching fraction is shared between the samples. The model used to describe the $m(K^+K^-\mu^+\mu^-)$ distribution is the same as for the $B_s^0 \to J/\psi\phi$ normalization mode. The model parameters for the signal component are fixed to those from the fit of the normalization mode, where the q^2 dependence of the mass resolution is accounted for with scaling factors determined from simulation.

Negligible contributions from physical background, including $B_s^0 \to K^+K^-\mu^+\mu^-$ decays with the K^+K^- system in an S-wave configuration, are not considered in the fit and a systematic uncertainty is assigned. Integrated over the full q^2 range, signal yields,

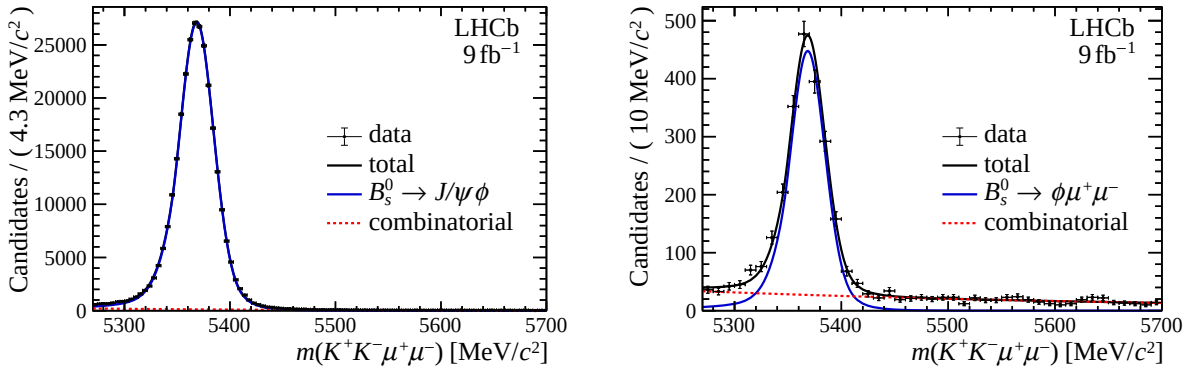

Figure 1: Reconstructed invariant mass of the $K^+K^-\mu^+\mu^-$ system for (left) the $B_s^0 \to J/\psi\phi$ normalization mode and (right) the $B_s^0 \to \phi\mu^+\mu^-$ signal candidates, integrated over q^2 and overlaid with the fit projections.

$N_{\phi\mu^+\mu^-}$, of 458 ± 12, 484 ± 13, and 1064 ± 28 are found from the simultaneous fit to the different data sets. Figure 1 (right) shows the $m(K^+K^-\mu^+\mu^-)$ distribution of the full data sample, integrated over q^2 and overlaid with the fit projections. Figures for the different data-taking periods are available as Supplemental Material.

The relative branching fraction measurement is affected by systematic uncertainties on the fit model and the efficiency ratio, where the latter is determined using SM simulation. A summary of the systematic uncertainties is provided in the Supplemental Material. The dominant systematic uncertainty on the absolute branching fraction (Eq. 1) originates from the model used to simulate $B_s^0 \to \phi\mu^+\mu^-$ events (0.04–$0.10 \times 10^{-8}\,\text{GeV}^{-2}c^4$). The model depends on $\Delta\Gamma_s$, the decay width difference in the B_s^0 system [31], and the specific form factors used. The effect of the model-choice on the relative efficiency is assessed by varying $\Delta\Gamma_s$ by 20%, corresponding to the difference in $\Delta\Gamma_s$ between the default value [32] and that of Ref. [26], and by comparing the form factors in Ref. [33] with the older calculations in Ref. [34]. The observed differences are taken as a systematic uncertainty. Other leading sources of systematic uncertainty arise from the limited size of the simulation sample (0.02–$0.07 \times 10^{-8}\,\text{GeV}^{-2}c^4$) and the omission of small background contributions from the fit model (0.01–$0.04 \times 10^{-8}\,\text{GeV}^{-2}c^4$).

The resulting relative and total branching fractions are given in Table 1. In addition, the differential branching fraction is shown in Fig. 2, overlaid with SM predictions. These predictions are based on form factor calculations using Light Cone Sum Rules (LCSRs) [33, 35] at low q^2 and Lattice QCD (LQCD) [36, 37] at high q^2, which are implemented in the FLAVIO software package [38]. In the q^2 region between 1.1 and $6.0\,\text{GeV}^2/c^4$, the measured branching fraction of $(2.88 \pm 0.22) \times 10^{-8}\,\text{GeV}^{-2}c^4$, lies $3.6\,\sigma$ below a precise SM prediction of $(5.37 \pm 0.66) \times 10^{-8}\,\text{GeV}^{-2}c^4$ which uses both LCSR and LQCD calculations. A less precise SM prediction of $(4.77 \pm 1.01) \times 10^{-8}\,\text{GeV}^{-2}c^4$ based on LCSRs alone lies $1.8\,\sigma$ above the measurement. To determine the total branching fraction, the branching fractions of the individual q^2 intervals are summed and corrected for the vetoed q^2 regions using $\epsilon_{q^2\,\text{veto}} = (65.47 \pm 0.27)\,\%$. This efficiency is determined using SM simulation, and its uncertainty originates from the comparison of form factors

Table 1: Differential $\mathrm{d}\mathcal{B}(B_s^0 \to \phi\mu^+\mu^-)/\mathrm{d}q^2$ branching fraction, both relative to the normalization mode and absolute, in intervals of q^2. The uncertainties are, in order, statistical, systematic, and due to the uncertainty on the branching fraction of the normalization mode.

q^2 interval $[\mathrm{GeV}^2/c^4]$	$\mathrm{d}\mathcal{B}(B_s^0 \to \phi\mu^+\mu^-)/\mathcal{B}(B_s^0 \to J/\psi\phi)\mathrm{d}q^2$ $[10^{-5}\,\mathrm{GeV}^{-2}c^4]$	$\mathrm{d}\mathcal{B}(B_s^0 \to \phi\mu^+\mu^-)/\mathrm{d}q^2$ $[10^{-8}\,\mathrm{GeV}^{-2}c^4]$
0.1–0.98	$7.61 \pm 0.52 \pm 0.12$	$7.74 \pm 0.53 \pm 0.12 \pm 0.37$
1.1–2.5	$3.09 \pm 0.29 \pm 0.07$	$3.15 \pm 0.29 \pm 0.07 \pm 0.15$
2.5–4.0	$2.30 \pm 0.25 \pm 0.05$	$2.34 \pm 0.26 \pm 0.05 \pm 0.11$
4.0–6.0	$3.05 \pm 0.24 \pm 0.06$	$3.11 \pm 0.24 \pm 0.06 \pm 0.15$
6.0–8.0	$3.10 \pm 0.23 \pm 0.06$	$3.15 \pm 0.24 \pm 0.06 \pm 0.15$
11.0–12.5	$4.69 \pm 0.30 \pm 0.07$	$4.78 \pm 0.30 \pm 0.08 \pm 0.23$
15.0–17.0	$5.15 \pm 0.28 \pm 0.10$	$5.25 \pm 0.29 \pm 0.10 \pm 0.25$
17.0–19.0	$4.12 \pm 0.29 \pm 0.12$	$4.19 \pm 0.29 \pm 0.12 \pm 0.20$
1.1–6.0	$2.83 \pm 0.15 \pm 0.05$	$2.88 \pm 0.15 \pm 0.05 \pm 0.14$
15.0–19.0	$4.55 \pm 0.20 \pm 0.11$	$4.63 \pm 0.20 \pm 0.11 \pm 0.22$

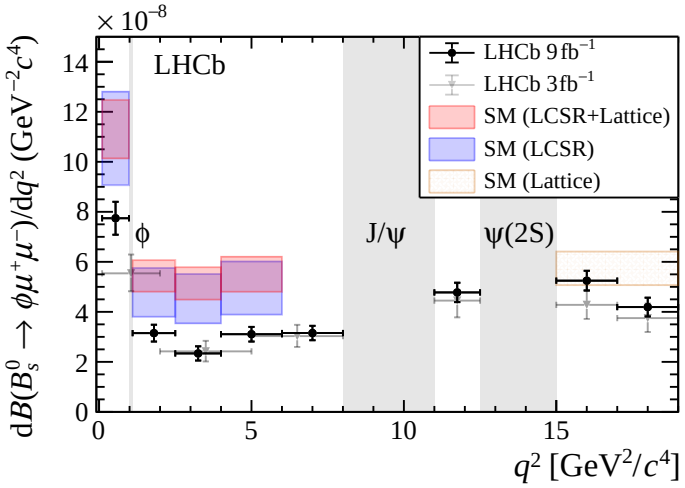

Figure 2: Differential branching fraction $\mathrm{d}\mathcal{B}(B_s^0 \to \phi\mu^+\mu^-)/\mathrm{d}q^2$, overlaid with SM predictions using Light Cone Sum Rules [33, 35, 38] at low q^2 and Lattice calculations [36, 37] at high q^2. The results from the LHCb $3\,\mathrm{fb}^{-1}$ analysis [1, 30] are shown with gray markers.

from Ref. [33] and Ref. [34]. The resulting branching fractions are

$$\frac{\mathcal{B}(B_s^0 \to \phi\mu^+\mu^-)}{\mathcal{B}(B_s^0 \to J/\psi\phi)} = (8.00 \pm 0.21 \pm 0.16 \pm 0.03) \times 10^{-4}\ ,$$
$$\mathcal{B}(B_s^0 \to \phi\mu^+\mu^-) = (8.14 \pm 0.21 \pm 0.16 \pm 0.03 \pm 0.39) \times 10^{-7},$$

where the uncertainties are, in order, statistical, systematic, from the extrapolation to the full q^2 region, and for the absolute branching fraction, from the branching fraction of the normalization mode.

The $B_s^0 \to f_2'\mu^+\mu^-$ decay is searched for using the combined q^2 region $[0.1, 0.98] \cup [1.1, 8.0] \cup [11.0, 12.5]\,\mathrm{GeV}^2/c^4$. The branching fraction of the signal decay is determined relative to the $B_s^0 \to J/\psi\phi$ normalization mode, according to

$$\frac{\mathcal{B}(B_s^0 \to f_2'\mu^+\mu^-)}{\mathcal{B}(B_s^0 \to J/\psi\phi)} = \mathcal{B}(J/\psi \to \mu^+\mu^-) \times \frac{\mathcal{B}(\phi \to K^+K^-)}{\mathcal{B}(f_2' \to K^+K^-)} \times \frac{N_{f_2'\mu^+\mu^-}}{N_{J/\psi\phi}} \times \frac{\epsilon_{J/\psi\phi}}{\epsilon_{f_2'\mu^+\mu^-}}, \qquad (2)$$

where the ratio of branching fractions $\mathcal{B}(\phi \to K^+K^-)/\mathcal{B}(f_2' \to K^+K^-) = 1.123 \pm 0.030$ [26] is used. To separate the f_2' signal from S- and P-wave contributions to the wide $m(K^+K^-)$ mass window, a two-dimensional fit to the $m(K^+K^-\mu^+\mu^-)$ and $m(K^+K^-)$ distributions is performed. The $B_s^0 \to f_2'\mu^+\mu^-$ signal decay is modeled in $m(K^+K^-\mu^+\mu^-)$ using the sum of two Gaussian functions with a power-law tail towards upper and lower mass, and in $m(K^+K^-)$ using a relativistic spin-2 Breit–Wigner function. The model parameters are determined from data using fits to the $B_s^0 \to J/\psi f_2'$ control mode and are fixed for the signal mode. Contributions from the S-wave and P-wave resonances, *e.g.* the ϕ and the $\phi(1680)$ mesons, are combined and described with a linear function in $m(K^+K^-)$ and use the same model as the signal in $m(K^+K^-\mu^+\mu^-)$. Interference effects are neglected as these were found to be small in the study of $B_s^0 \to J/\psi K^+K^-$ decays in Ref. [39]. The combinatorial background is modeled using an exponential function in both the reconstructed B_s^0 mass and the mass of the dikaon system. Background from $B^0 \to K^+\pi^-\mu^+\mu^-$ and $\Lambda_b^0 \to pK^-\mu^+\mu^-$ decays is found to be non-negligible in the wide $m(K^+K^-)$ window. These background components are included in the fit model, with their yields constrained to the expected values and line shapes determined on simulated events.

The branching fraction of the $B_s^0 \to f_2'\mu^+\mu^-$ decay is determined using a simultaneous fit to the three data samples. The branching fraction of the signal and the S- and P-wave contributions are shared between the data samples. From this fit, the signal yields, $N_{f_2'\mu^+\mu^-}$, are found to be 62 ± 8, 67 ± 8, and 161 ± 20 for the different data-taking periods. Figure 3 shows the $m(K^+K^-\mu^+\mu^-)$ and $m(K^+K^-)$ mass distributions, where the latter is shown within $50\,\mathrm{MeV}/c^2$ of the known B_s^0 mass [26], overlaid with the fit projections. The significance of the signal is determined using Wilks' theorem [40], comparing the log–likelihood with and without the signal component. The $B_s^0 \to f_2'\mu^+\mu^-$ decay is observed with a statistical significance of $9\,\sigma$. Systematic effects on the significance due to the choice of fit model are negligible.

The dominant systematic uncertainties on the relative branching fraction of the $B_s^0 \to f_2'\mu^+\mu^-$ decay originate from the uncertainty of the branching fraction ratio $\mathcal{B}(\phi \to K^+K^-)/\mathcal{B}(f_2' \to K^+K^-)$ (0.04×10^{-7}), the modeling of the parameters of the Breit–Wigner function describing the f_2' resonance, and the simplified fit model for the $m(K^+K^-)$ distribution (0.03×10^{-7}). The effect of the simplified fit model is evaluated using pseudoexperiments, in which events are generated using the amplitude model in Ref. [39] and fit with the default model. The observed difference in the determined yield is taken as a systematic uncertainty. Further details on the systematic uncertainties associated with $\mathcal{B}(B_s^0 \to f_2'\mu^+\mu^-)$ are given in the Supplemental Material.

The fraction of signal events within the considered q^2 region is calculated using the q^2-differential distribution in Ref. [41] and found to be $\epsilon_{q^2\,\mathrm{veto}} = (73.8 \pm 2.8)\,\%$. Accounting

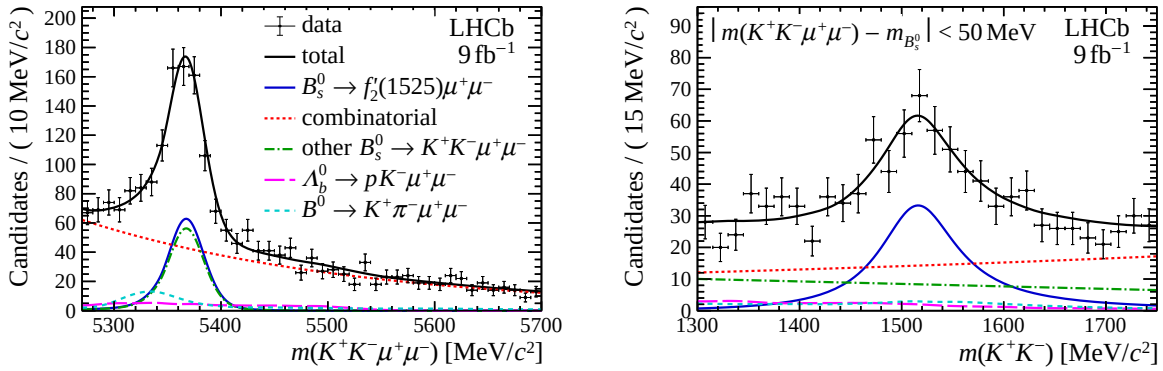

Figure 3: Reconstructed invariant mass of (left) the $K^+K^-\mu^+\mu^-$ system and (right) the K^+K^- system for $B_s^0 \to f_2'\mu^+\mu^-$ candidates, overlaid with the fit projections. The $m(K^+K^-)$ distribution is shown in the B_s^0 signal region $\pm 50\,\text{MeV}/c^2$ around the known B_s^0 mass.

for this factor, the relative and total branching fractions are determined to be

$$\frac{\mathcal{B}(B_s^0 \to f_2'\mu^+\mu^-)}{\mathcal{B}(B_s^0 \to J/\psi\phi)} = (1.55 \pm 0.19 \pm 0.06 \pm 0.06) \times 10^{-4} \,,$$
$$\mathcal{B}(B_s^0 \to f_2'\mu^+\mu^-) = (1.57 \pm 0.19 \pm 0.06 \pm 0.06 \pm 0.08) \times 10^{-7} \,,$$

where the given uncertainties are, in order, statistical, systematic, from the extrapolation to the full q^2 range and, for the absolute branching fraction, from the uncertainty on the branching fraction of the normalization mode. The total $B_s^0 \to f_2'\mu^+\mu^-$ branching fraction is found to be in agreement with SM predictions [41–43].

In summary, the most precise measurement of the branching fraction of the rare $B_s^0 \to \phi\mu^+\mu^-$ decay is presented, using LHCb data corresponding to an integrated luminosity of $9\,\text{fb}^{-1}$. Consistent with earlier measurements [1, 2], the data are found to lie below SM expectations. In the q^2 region between 1.1 and $6.0\,\text{GeV}^2/c^4$ the measurement deviates by $3.6\,\sigma$ with respect to a precise SM prediction [33, 35–38]. These results supersede, and are consistent with, those of Refs. [1, 2]. In addition, the first observation of the rare $B_s^0 \to f_2'\mu^+\mu^-$ decay is reported with a statistical significance of nine standard deviations and the resulting branching fraction is found to be in agreement with SM predictions [41–43].

Acknowledgements

We express our gratitude to our colleagues in the CERN accelerator departments for the excellent performance of the LHC. We thank the technical and administrative staff at the LHCb institutes. We acknowledge support from CERN and from the national agencies: CAPES, CNPq, FAPERJ and FINEP (Brazil); MOST and NSFC (China); CNRS/IN2P3 (France); BMBF, DFG and MPG (Germany); INFN (Italy); NWO (Netherlands); MNiSW and NCN (Poland); MEN/IFA (Romania); MSHE (Russia); MICINN (Spain); SNSF and SER (Switzerland); NASU (Ukraine); STFC (United Kingdom); DOE NP and NSF (USA). We acknowledge the computing resources that are provided by CERN, IN2P3 (France), KIT and DESY (Germany), INFN (Italy), SURF (Netherlands), PIC (Spain), GridPP (United Kingdom), RRCKI and Yandex LLC (Russia), CSCS (Switzerland),

IFIN-HH (Romania), CBPF (Brazil), PL-GRID (Poland) and NERSC (USA). We are indebted to the communities behind the multiple open-source software packages on which we depend. Individual groups or members have received support from ARC and ARDC (Australia); AvH Foundation (Germany); EPLANET, Marie Skłodowska-Curie Actions and ERC (European Union); A*MIDEX, ANR, IPhU and Labex P2IO, and Région Auvergne-Rhône-Alpes (France); Key Research Program of Frontier Sciences of CAS, CAS PIFI, CAS CCEPP, Fundamental Research Funds for the Central Universities, and Sci. & Tech. Program of Guangzhou (China); RFBR, RSF and Yandex LLC (Russia); GVA, XuntaGal and GENCAT (Spain); the Leverhulme Trust, the Royal Society and UKRI (United Kingdom).

Supplemental material

Supplemental figures

Figure 4 shows the $K^+K^-\mu^+\mu^-$ invariant mass versus q^2 for selected (top) $B_s^0 \to \phi\mu^+\mu^-$ and (bottom) $B_s^0 \to f_2'\mu^+\mu^-$ candidates. The signal modes are clearly visible as a vertical band around the known mass of the B_s^0 meson.

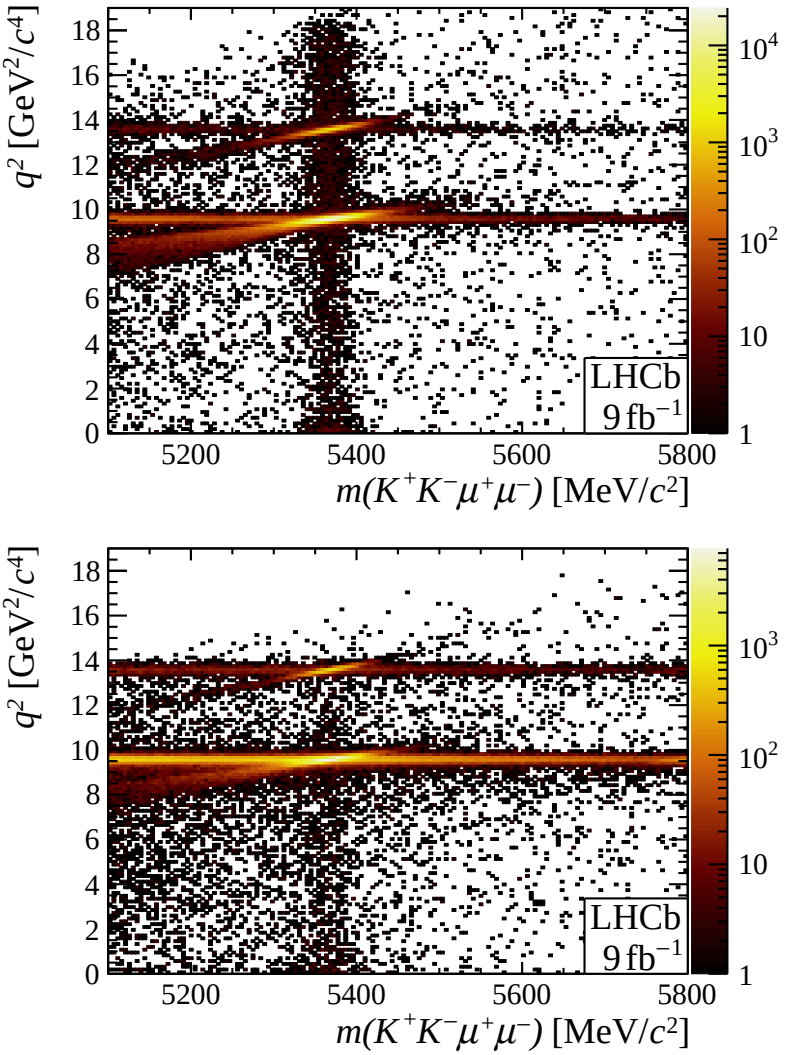

Figure 4: Invariant mass of the $K^+K^-\mu^+\mu^-$ system versus q^2 for selected (top) $B_s^0 \to \phi\mu^+\mu^-$ and (bottom) $B_s^0 \to f_2'\mu^+\mu^-$ candidates across all data-taking periods.

The $K^+K^-\mu^+\mu^-$ invariant mass of the selected (left) $B_s^0 \to J/\psi\phi$ and (right) $B_s^0 \to \phi\mu^+\mu^-$ candidates, integrated over q^2, is shown in Fig. 5 for the different data-taking periods. The total fit projection (black line) is overlaid on the data, along with the signal component (blue line) and background component describing combinatorial background (red dotted line).

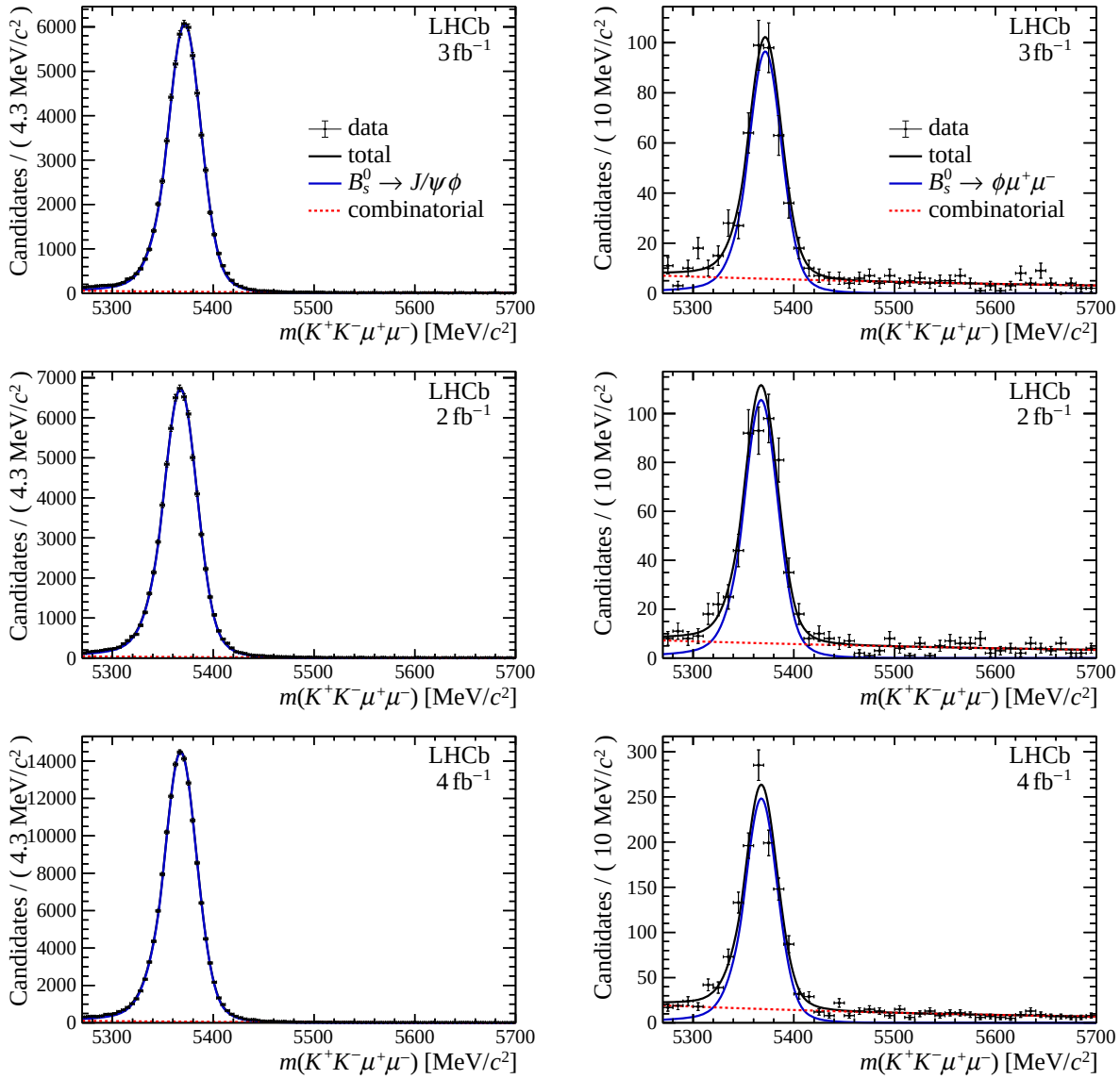

Figure 5: Reconstructed invariant mass of the $K^+K^-\mu^+\mu^-$ system for (left) $B_s^0 \to J/\psi\phi$ and (right) $B_s^0 \to \phi\mu^+\mu^-$ candidates, integrated over q^2, for the (top) 2011–2012, (middle) 2015–2016, and (bottom) 2017–2018 data-taking periods. The data are overlaid with the fit projections.

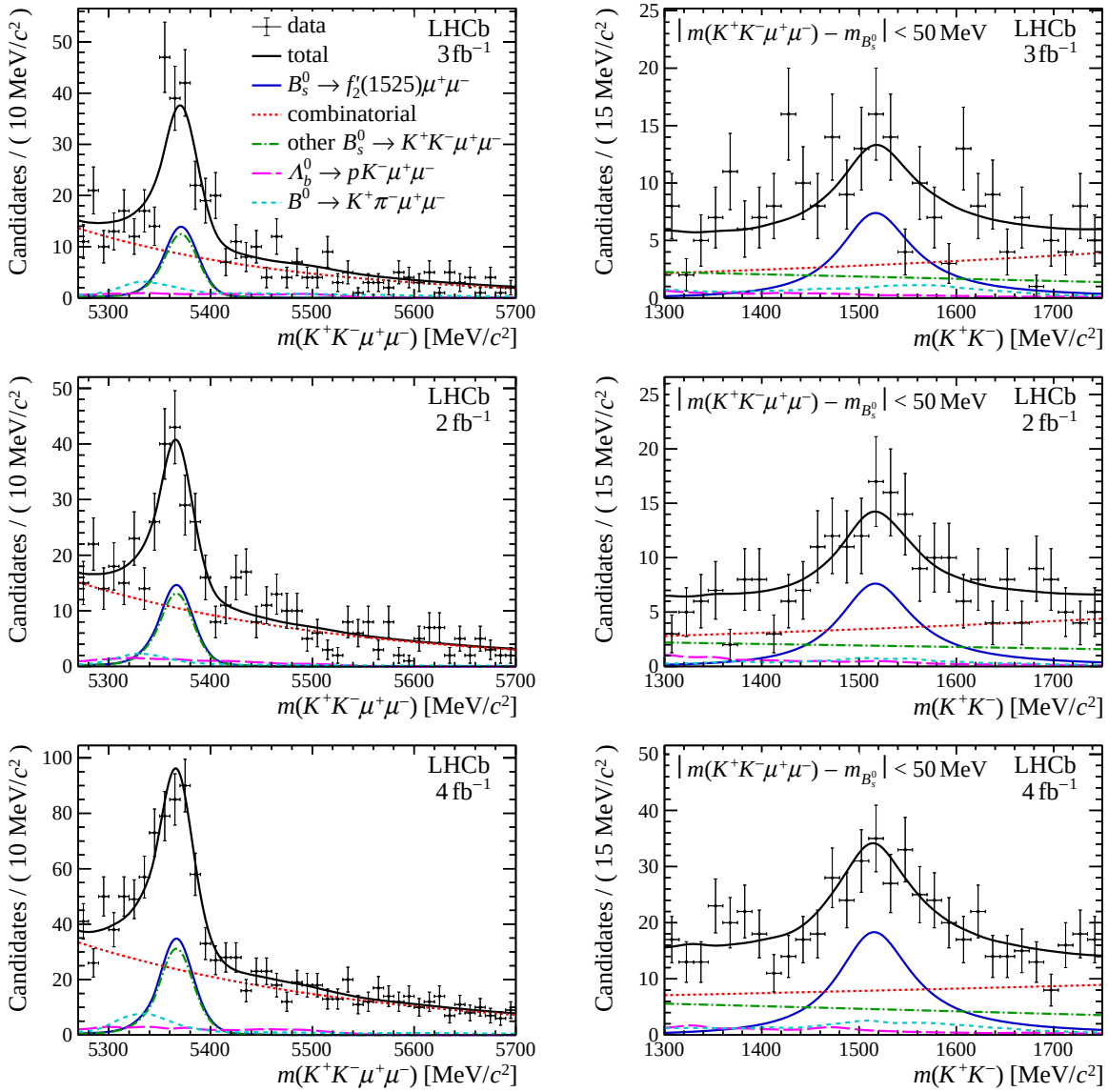

Figure 6: Reconstructed invariant mass of (left) the $K^+K^-\mu^+\mu^-$ system and (right) the K^+K^- system for $B_s^0 \to f_2'\mu^+\mu^-$ candidates for the (top) 2011–2012, (middle) 2015–2016, and (bottom) 2017–2018 data-taking periods. Distributions are overlaid with the fit projections. The K^+K^- distribution is shown in the B_s^0 signal region ± 50 MeV around the known B_s^0 mass.

Figure 6 shows the (left) $K^+K^-\mu^+\mu^-$ and (right) K^+K^- invariant mass distributions of selected $B_s^0 \to f_2'\mu^+\mu^-$ candidates for the different data-taking periods. The total fit projection (black line) is overlaid on the data along with projections of individual fit components describing: the signal (blue line), other $B_s^0 \to K^+K^-\mu^+\mu^-$ decays (green dash-dotted line), combinatorial background (red dotted line) and Λ_b^0 (magenta long dashed line) and B^0 (cyan medium size dashed line) decays.

Systematic uncertainties

The systematic uncertainties associated with the measurement of the branching fractions of the $B_s^0 \to \phi\mu^+\mu^-$ and $B_s^0 \to f_2'\mu^+\mu^-$ decays are summarized in Table 2. The *Physics model* in Table 2 refers to the model used for the generation of $B_s^0 \to \phi\mu^+\mu^-$ and $B_s^0 \to f_2'\mu^+\mu^-$ decays in simulation. Studied variations to the $B_s^0 \to \phi\mu^+\mu^-$ physics model are detailed in the Letter. The model used for $B_s^0 \to f_2'\mu^+\mu^-$ decays accounts only for phase-space effects. The q^2 distribution is therefore not an exact description of data and is corrected to the predictions in Ref. [41]. The difference in the relative efficiency with and without this correction is assigned as a systematic uncertainty.

The *Residual background* in Table 2 refers to contamination of the signal modes from residual physical background. Background contributions to $B_s^0 \to \phi\mu^+\mu^-$ decays are neglected in the fit and a systematic uncertainty is assigned. For $B_s^0 \to f_2'\mu^+\mu^-$ decays, a systematic uncertainty is associated with the choice of lineshape used to describe background from $B^0 \to K^+\pi^-\mu^+\mu^-$ and $\Lambda_b^0 \to pK^-\mu^+\mu^-$ decays in the fit.

The systematic uncertainty associated with the $B_s^0 \to \phi\mu^+\mu^-$ *signal fit model* in Table 2 is obtained using an alternative description for the radiative tail of the B_s^0 meson. For the $B_s^0 \to f_2'\mu^+\mu^-$ decay, the lineshape in $m(K^+K^-)$ of both the non-signal $B_s^0 \to K^+K^-\mu^+\mu^-$ contributions and the signal decay are varied. For the $B_s^0 \to K^+K^-\mu^+\mu^-$ contributions, an alternative description is taken from Ref. [39], as detailed in the Letter. For the f_2' lineshape, the input values for the Blatt–Weisskopf barrier functions [44] are varied, namely the barrier radius of the f_2' and B_s^0 mesons, along with the orbital angular momentum of the B_s^0 meson.

The *simulation corrections* in Table 2 refer to the uncertainties associated with applied corrections to simulated events. Corrections are recalculated using alternative binning schemes or accounting for the finite statistics of the control modes used to derive the corrections. The uncertainty associated with small levels of mismodelling in distributions which are not directly corrected for in the default approach (e.g. tracking efficiencies) are indicated under *residual mismodelling*.

Table 2: Systematic uncertainties on the differential branching fraction $\mathrm{d}\mathcal{B}(B_s^0 \to \phi\mu^+\mu^-)/\mathrm{d}q^2$ and on the total branching fraction $\mathcal{B}(B_s^0 \to f_2'\mu^+\mu^-)$. Ranges indicate the variation across the q^2 intervals. The uncertainty from the branching fraction of the normalization mode, $\mathcal{B}(B_s^0 \to J/\psi\phi)$, is quoted separately.

Source	$\sigma_{\text{syst.}}\big(\mathrm{d}\mathcal{B}(B_s^0 \to \phi\mu^+\mu^-)/\mathrm{d}q^2\big)$ $[10^{-8}\,\text{GeV}^{-2}c^4]$	$\sigma_{\text{syst.}}\big(\mathcal{B}(B_s^0 \to f_2'\mu^+\mu^-)\big)$ $[10^{-7}]$
Physics model	0.04–0.10	0.02
Limited simulation sample	0.02–0.07	0.01
Residual background	0.01–0.04	0.01
Fit bias	0.00–0.03	< 0.01
Signal fit model	0.00–0.01	0.03
Simulation corrections	0.00–0.03	0.01
Residual mismodelling	0.00–0.02	< 0.01
$\mathcal{B}(J/\psi \to \mu^+\mu^-)$	0.01–0.04	0.01
$\mathcal{B}(\phi \to K^+K^-)/\mathcal{B}(f_2' \to K^+K^-)$	–	0.04
Quadratic sum	0.05–0.12	0.06
Normalization $\mathcal{B}(B_s^0 \to J/\psi\phi)$	0.11–0.37	0.07

References

[1] LHCb collaboration, R. Aaij *et al.*, *Angular analysis and differential branching fraction of the decay* $B_s^0 \to \phi\mu^+\mu^-$, JHEP **09** (2015) 179, arXiv:1506.08777.

[2] LHCb collaboration, R. Aaij *et al.*, *Differential branching fraction and angular analysis of the decay* $B_s^0 \to \phi\mu^+\mu^-$, JHEP **07** (2013) 084, arXiv:1305.2168.

[3] LHCb collaboration, R. Aaij *et al.*, *Measurements of the S-wave fraction in* $B^0 \to K^+\pi^-\mu^+\mu^-$ *decays and the* $B^0 \to K^*(892)^0\mu^+\mu^-$ *differential branching fraction*, JHEP **11** (2016) 047, Erratum ibid. **04** (2017) 142, arXiv:1606.04731.

[4] LHCb collaboration, R. Aaij *et al.*, *Differential branching fraction and angular analysis of* $\Lambda_b^0 \to \Lambda\mu^+\mu^-$ *decays*, JHEP **06** (2015) 115, Erratum ibid. **09** (2018) 145, arXiv:1503.07138.

[5] LHCb collaboration, R. Aaij *et al.*, *Differential branching fractions and isospin asymmetries of* $B \to K^{(*)}\mu^+\mu^-$ *decays*, JHEP **06** (2014) 133, arXiv:1403.8044.

[6] LHCb collaboration, R. Aaij *et al.*, *Measurement of CP-averaged observables in the* $B^0 \to K^{*0}\mu^+\mu^-$ *decay*, Phys. Rev. Lett. **125** (2020) 011802, arXiv:2003.04831.

[7] LHCb collaboration, R. Aaij *et al.*, *Angular analysis of the* $B^0 \to K^{*0}\mu^+\mu^-$ *decay using* $3\,fb^{-1}$ *of integrated luminosity*, JHEP **02** (2016) 104, arXiv:1512.04442.

[8] ATLAS collaboration, M. Aaboud *et al.*, *Angular analysis of* $B_d^0 \to K^*\mu^+\mu^-$ *decays in pp collisions at* $\sqrt{s} = 8$ *TeV with the ATLAS detector*, JHEP **10** (2018) 047, arXiv:1805.04000.

[9] CMS collaboration, V. Khachatryan *et al.*, *Angular analysis of the decay* $B^0 \to K^{*0}\mu^+\mu^-$ *from pp collisions at* $\sqrt{s} = 8$ *TeV*, Phys. Lett. **B753** (2016) 424, arXiv:1507.08126.

[10] CMS collaboration, A. M. Sirunyan *et al.*, *Measurement of angular parameters from the decay* $\mathrm{B}^0 \to \mathrm{K}^{*0}\mu^+\mu^-$ *in proton-proton collisions at* $\sqrt{s} = 8$ *TeV*, Phys. Lett. **B781** (2018) 517, arXiv:1710.02846.

[11] Belle collaboration, S. Wehle *et al.*, *Lepton-flavor-dependent angular analysis of* $B \to K^*\ell^+\ell^-$, Phys. Rev. Lett. **118** (2017) 111801, arXiv:1612.05014.

[12] LHCb collaboration, R. Aaij *et al.*, *Test of lepton universality in beauty-quark decays*, arXiv:2103.11769, Submitted to Nature Physics.

[13] LHCb collaboration, R. Aaij *et al.*, *Test of lepton universality using* $\Lambda_b^0 \to pK^-\ell^+\ell^-$ *decays*, JHEP **05** (2020) 040, arXiv:1912.08139.

[14] LHCb collaboration, R. Aaij *et al.*, *Search for lepton-universality violation in* $B^+ \to K^+\ell^+\ell^-$ *decays*, Phys. Rev. Lett. **122** (2019) 191801, arXiv:1903.09252.

[15] LHCb collaboration, R. Aaij *et al.*, *Test of lepton universality with* $B^0 \to K^{*0}\ell^+\ell^-$ *decays*, JHEP **08** (2017) 055, arXiv:1705.05802.

[16] LHCb collaboration, R. Aaij *et al.*, *Test of lepton universality using $B^+ \to K^+\ell^+\ell^-$ decays*, Phys. Rev. Lett. **113** (2014) 151601, arXiv:1406.6482.

[17] BaBar collaboration, J. P. Lees *et al.*, *Measurement of branching fractions and rate asymmetries in the rare decays $B \to K^{(*)}l^+l^-$*, Phys. Rev. **D86** (2012) 032012, arXiv:1204.3933.

[18] Belle collaboration, S. Choudhury *et al.*, *Test of lepton flavor universality and search for lepton flavor violation in $B \to K\ell\ell$ decays*, JHEP **03** (2021) 105, arXiv:1908.01848.

[19] Belle collaboration, A. Abdesselam *et al.*, *Test of lepton-flavor universality in $B \to K^*\ell^+\ell^-$ decays at Belle*, Phys. Rev. Lett. **126** (2021) 161801, arXiv:1904.02440.

[20] LHCb collaboration, A. A. Alves Jr. *et al.*, *The LHCb detector at the LHC*, JINST **3** (2008) S08005.

[21] LHCb collaboration, R. Aaij *et al.*, *LHCb detector performance*, Int. J. Mod. Phys. **A30** (2015) 1530022, arXiv:1412.6352.

[22] R. Aaij *et al.*, *The LHCb trigger and its performance in 2011*, JINST **8** (2013) P04022, arXiv:1211.3055.

[23] T. Sjöstrand, S. Mrenna, and P. Skands, *A brief introduction to PYTHIA 8.1*, Comput. Phys. Commun. **178** (2008) 852, arXiv:0710.3820.

[24] D. J. Lange, *The EvtGen particle decay simulation package*, Nucl. Instrum. Meth. **A462** (2001) 152.

[25] Geant4 collaboration, J. Allison *et al.*, *Geant4 developments and applications*, IEEE Trans. Nucl. Sci. **53** (2006) 270; Geant4 collaboration, S. Agostinelli *et al.*, *Geant4: A simulation toolkit*, Nucl. Instrum. Meth. **A506** (2003) 250.

[26] Particle Data Group, P. A. Zyla *et al.*, *Review of particle physics*, Prog. Theor. Exp. Phys. **2020** (2020) 083C01.

[27] L. Breiman, J. H. Friedman, R. A. Olshen, and C. J. Stone, *Classification and regression trees*, Wadsworth international group, Belmont, California, USA, 1984.

[28] Y. Freund and R. E. Schapire, *A decision-theoretic generalization of on-line learning and an application to boosting*, J. Comput. Syst. Sci. **55** (1997) 119.

[29] A. Blum, A. Kalai, and J. Langford, *Beating the hold-out: Bounds for k-fold and progressive cross-validation*, in *Proceedings of the Twelfth Annual Conference on Computational Learning Theory*, COLT '99, (New York, NY, USA), 203–208, ACM, 1999.

[30] LHCb collaboration, R. Aaij *et al.*, *Precise measurement of the f_s/f_d ratio of fragmentation fractions and of B^0_s decay branching fractions*, Phys. Rev. **D104** (2021) 032005, arXiv:2103.06810.

[31] S. Descotes-Genon and J. Virto, *Time dependence in $B \to V\ell\ell$ decays*, JHEP **04** (2015) 045, arXiv:1502.05509, Erratum: JHEP **07** (2015) 049.

[32] Particle Data Group, K. A. Olive *et al.*, *Review of particle physics*, Chin. Phys. **C38** (2014) 090001.

[33] A. Bharucha, D. M. Straub, and R. Zwicky, *$B \to V\ell^+\ell^-$ in the Standard Model from light-cone sum rules*, JHEP **08** (2016) 098, arXiv:1503.05534.

[34] P. Ball and R. Zwicky, *$B_{d,s} \to \rho, \omega, K^*, \phi$ decay form-factors from light-cone sum rules revisited*, Phys. Rev. **D71** (2005) 014029, arXiv:hep-ph/0412079.

[35] W. Altmannshofer and D. M. Straub, *New physics in $b \to s$ transitions after LHC Run 1*, Eur. Phys. J. **C75** (2015) 382, arXiv:1411.3161.

[36] R. R. Horgan, Z. Liu, S. Meinel, and M. Wingate, *Calculation of $B^0 \to K^{*0}\mu^+\mu^-$ and $B_s^0 \to \phi\mu^+\mu^-$ observables using form factors from lattice QCD*, Phys. Rev. Lett. **112** (2014) 212003, arXiv:1310.3887.

[37] R. R. Horgan, Z. Liu, S. Meinel, and M. Wingate, *Rare B decays using lattice QCD form factors*, PoS **LATTICE2014** (2015) 372, arXiv:1501.00367.

[38] D. M. Straub, *flavio: a Python package for flavour and precision phenomenology in the Standard Model and beyond*, arXiv:1810.08132.

[39] LHCb collaboration, R. Aaij *et al.*, *Resonances and CP-violation in B_s^0 and $\overline{B}_s^0 \to J/\psi K^+K^-$ decays in the mass region above the $\phi(1020)$*, JHEP **08** (2017) 037, arXiv:1704.08217.

[40] S. S. Wilks, *The large-sample distribution of the likelihood ratio for testing composite hypotheses*, Ann. Math. Stat. **9** (1938) 60.

[41] N. Rajeev, N. Sahoo, and R. Dutta, *Angular analysis of $B_s \to f_2'(1525)(\to K^+K^-)\mu^+\mu^-$ decays as a probe to lepton flavor universality violation*, Phys. Rev. D **103** (2021) 095007.

[42] R.-H. Li, C.-D. Lu, and W. Wang, *Branching ratios, forward-backward asymmetries and angular distributions of $B \to K_2^* l^+ l^-$ in the standard model and new physics scenarios*, Phys. Rev. **D83** (2011) 034034, arXiv:1012.2129.

[43] Y.-B. Zuo *et al.*, *$B_{(s)}$ to light tensor meson form factors via LCSR in HQEFT with applications to semileptonic decays*, Eur. Phys. J. **C81** (2021) 30.

[44] J. M. Blatt and V. F. Weisskopf, *Theoretical nuclear physics*, Springer, New York, 1952.

LHCb collaboration

R. Aaij[32], C. Abellán Beteta[50], T. Ackernley[60], B. Adeva[46], M. Adinolfi[54], H. Afsharnia[9], C.A. Aidala[86], S. Aiola[25], Z. Ajaltouni[9], S. Akar[65], J. Albrecht[15], F. Alessio[48], M. Alexander[59], A. Alfonso Albero[45], Z. Aliouche[62], G. Alkhazov[38], P. Alvarez Cartelle[55], S. Amato[2], Y. Amhis[11], L. An[48], L. Anderlini[22], A. Andreianov[38], M. Andreotti[21], F. Archilli[17], A. Artamonov[44], M. Artuso[68], K. Arzymatov[42], E. Aslanides[10], M. Atzeni[50], B. Audurier[12], S. Bachmann[17], M. Bachmayer[49], J.J. Back[56], P. Baladron Rodriguez[46], V. Balagura[12], W. Baldini[21], J. Baptista Leite[1], R.J. Barlow[62], S. Barsuk[11], W. Barter[61], M. Bartolini[24], F. Baryshnikov[83], J.M. Basels[14], G. Bassi[29], B. Batsukh[68], A. Battig[15], A. Bay[49], M. Becker[15], F. Bedeschi[29], I. Bediaga[1], A. Beiter[68], V. Belavin[42], S. Belin[27], V. Bellee[49], K. Belous[44], I. Belov[40], I. Belyaev[41], G. Bencivenni[23], E. Ben-Haim[13], A. Berezhnoy[40], R. Bernet[50], D. Berninghoff[17], H.C. Bernstein[68], C. Bertella[48], A. Bertolin[28], C. Betancourt[50], F. Betti[48], Ia. Bezshyiko[50], S. Bhasin[54], J. Bhom[35], L. Bian[73], M.S. Bieker[15], S. Bifani[53], P. Billoir[13], M. Birch[61], F.C.R. Bishop[55], A. Bitadze[62], A. Bizzeti[22,k], M. Bjørn[63], M.P. Blago[48], T. Blake[56], F. Blanc[49], S. Blusk[68], D. Bobulska[59], J.A. Boelhauve[15], O. Boente Garcia[46], T. Boettcher[65], A. Boldyrev[82], A. Bondar[43], N. Bondar[38,48], S. Borghi[62], M. Borisyak[42], M. Borsato[17], J.T. Borsuk[35], S.A. Bouchiba[49], T.J.V. Bowcock[60], A. Boyer[48], C. Bozzi[21], M.J. Bradley[61], S. Braun[66], A. Brea Rodriguez[46], M. Brodski[48], J. Brodzicka[35], A. Brossa Gonzalo[56], D. Brundu[27], A. Buonaura[50], C. Burr[48], A. Bursche[72], A. Butkevich[39], J.S. Butter[32], J. Buytaert[48], W. Byczynski[48], S. Cadeddu[27], H. Cai[73], R. Calabrese[21,f], L. Calefice[15,13], L. Calero Diaz[23], S. Cali[23], R. Calladine[53], M. Calvi[26,j], M. Calvo Gomez[85], P. Camargo Magalhaes[54], P. Campana[23], A.F. Campoverde Quezada[6], S. Capelli[26,j], L. Capriotti[20,d], A. Carbone[20,d], G. Carboni[31], R. Cardinale[24], A. Cardini[27], I. Carli[4], P. Carniti[26,j], L. Carus[14], K. Carvalho Akiba[32], A. Casais Vidal[46], G. Casse[60], M. Cattaneo[48], G. Cavallero[48], S. Celani[49], J. Cerasoli[10], A.J. Chadwick[60], M.G. Chapman[54], M. Charles[13], Ph. Charpentier[48], G. Chatzikonstantinidis[53], C.A. Chavez Barajas[60], M. Chefdeville[8], C. Chen[3], S. Chen[4], A. Chernov[35], V. Chobanova[46], S. Cholak[49], M. Chrzaszcz[35], A. Chubykin[38], V. Chulikov[38], P. Ciambrone[23], M.F. Cicala[56], X. Cid Vidal[46], G. Ciezarek[48], P.E.L. Clarke[58], M. Clemencic[48], H.V. Cliff[55], J. Closier[48], J.L. Cobbledick[62], V. Coco[48], J.A.B. Coelho[11], J. Cogan[10], E. Cogneras[9], L. Cojocariu[37], P. Collins[48], T. Colombo[48], L. Congedo[19,c], A. Contu[27], N. Cooke[53], G. Coombs[59], I. Corredoira Fernandez[46], G. Corti[48], C.M. Costa Sobral[56], B. Couturier[48], D.C. Craik[64], J. Crkovská[67], M. Cruz Torres[1], R. Currie[58], C.L. Da Silva[67], S. Dadabaev[83], E. Dall'Occo[15], J. Dalseno[46], C. D'Ambrosio[48], A. Danilina[41], P. d'Argent[48], A. Davis[62], O. De Aguiar Francisco[62], K. De Bruyn[79], S. De Capua[62], M. De Cian[49], J.M. De Miranda[1], L. De Paula[2], M. De Serio[19,c], D. De Simone[50], P. De Simone[23], J.A. de Vries[80], C.T. Dean[67], D. Decamp[8], L. Del Buono[13], B. Delaney[55], H.-P. Dembinski[15], A. Dendek[34], V. Denysenko[50], D. Derkach[82], O. Deschamps[9], F. Desse[11], F. Dettori[27,e], B. Dey[77], A. Di Cicco[23], P. Di Nezza[23], S. Didenko[83], L. Dieste Maronas[46], H. Dijkstra[48], V. Dobishuk[52], A.M. Donohoe[18], F. Dordei[27], A.C. dos Reis[1], L. Douglas[59], A. Dovbnya[51], A.G. Downes[8], K. Dreimanis[60], M.W. Dudek[35], L. Dufour[48], V. Duk[78], P. Durante[48], J.M. Durham[67], D. Dutta[62], A. Dziurda[35], A. Dzyuba[38], S. Easo[57], U. Egede[69], V. Egorychev[41], S. Eidelman[43,v], S. Eisenhardt[58], S. Ek-In[49], L. Eklund[59,w], S. Ely[68], A. Ene[37], E. Epple[67], S. Escher[14], J. Eschle[50], S. Esen[13], T. Evans[48], A. Falabella[20], J. Fan[3], Y. Fan[6], B. Fang[73], S. Farry[60], D. Fazzini[26,j], M. Féo[48], A. Fernandez Prieto[46], J.M. Fernandez-tenllado Arribas[45], A.D. Fernez[66], F. Ferrari[20,d], L. Ferreira Lopes[49], F. Ferreira Rodrigues[2], S. Ferreres Sole[32], M. Ferrillo[50], M. Ferro-Luzzi[48], S. Filippov[39], R.A. Fini[19], M. Fiorini[21,f], M. Firlej[34], K.M. Fischer[63], D.S. Fitzgerald[86], C. Fitzpatrick[62], T. Fiutowski[34], A. Fkiaras[48], F. Fleuret[12], M. Fontana[13], F. Fontanelli[24,h], R. Forty[48], V. Franco Lima[60], M. Franco Sevilla[66], M. Frank[48], E. Franzoso[21], G. Frau[17], C. Frei[48],

D.A. Friday[59], J. Fu[25], Q. Fuehring[15], W. Funk[48], E. Gabriel[32], T. Gaintseva[42], A. Gallas Torreira[46], D. Galli[20,d], S. Gambetta[58,48], Y. Gan[3], M. Gandelman[2], P. Gandini[25], Y. Gao[5], M. Garau[27], L.M. Garcia Martin[56], P. Garcia Moreno[45], J. García Pardiñas[26,j], B. Garcia Plana[46], F.A. Garcia Rosales[12], L. Garrido[45], C. Gaspar[48], R.E. Geertsema[32], D. Gerick[17], L.L. Gerken[15], E. Gersabeck[62], M. Gersabeck[62], T. Gershon[56], D. Gerstel[10], Ph. Ghez[8], V. Gibson[55], H.K. Giemza[36], M. Giovannetti[23,p], A. Gioventù[46], P. Gironella Gironell[45], L. Giubega[37], C. Giugliano[21,f,48], K. Gizdov[58], E.L. Gkougkousis[48], V.V. Gligorov[13], C. Göbel[70], E. Golobardes[85], D. Golubkov[41], A. Golutvin[61,83], A. Gomes[1,a], S. Gomez Fernandez[45], F. Goncalves Abrantes[63], M. Goncerz[35], G. Gong[3], P. Gorbounov[41], I.V. Gorelov[40], C. Gotti[26], E. Govorkova[48], J.P. Grabowski[17], T. Grammatico[13], L.A. Granado Cardoso[48], E. Graugés[45], E. Graverini[49], G. Graziani[22], A. Grecu[37], L.M. Greeven[32], P. Griffith[21,f], L. Grillo[62], S. Gromov[83], B.R. Gruberg Cazon[63], C. Gu[3], M. Guarise[21], P. A. Günther[17], E. Gushchin[39], A. Guth[14], Y. Guz[44], T. Gys[48], T. Hadavizadeh[69], G. Haefeli[49], C. Haen[48], J. Haimberger[48], T. Halewood-leagas[60], P.M. Hamilton[66], J.P. Hammerich[60], Q. Han[7], X. Han[17], T.H. Hancock[63], S. Hansmann-Menzemer[17], N. Harnew[63], T. Harrison[60], C. Hasse[48], M. Hatch[48], J. He[6,b], M. Hecker[61], K. Heijhoff[32], K. Heinicke[15], A.M. Hennequin[48], K. Hennessy[60], L. Henry[48], J. Heuel[14], A. Hicheur[2], D. Hill[49], M. Hilton[62], S.E. Hollitt[15], J. Hu[17], J. Hu[72], W. Hu[7], X. Hu[3], W. Huang[6], X. Huang[73], W. Hulsbergen[32], R.J. Hunter[56], M. Hushchyn[82], D. Hutchcroft[60], D. Hynds[32], P. Ibis[15], M. Idzik[34], D. Ilin[38], P. Ilten[65], A. Inglessi[38], A. Ishteev[83], K. Ivshin[38], R. Jacobsson[48], S. Jakobsen[48], E. Jans[32], B.K. Jashal[47], A. Jawahery[66], V. Jevtic[15], M. Jezabek[35], F. Jiang[3], M. John[63], D. Johnson[48], C.R. Jones[55], T.P. Jones[56], B. Jost[48], N. Jurik[48], S. Kandybei[51], Y. Kang[3], M. Karacson[48], M. Karpov[82], F. Keizer[48], M. Kenzie[56], T. Ketel[33], B. Khanji[15], A. Kharisova[84], S. Kholodenko[44], T. Kirn[14], V.S. Kirsebom[49], O. Kitouni[64], S. Klaver[32], K. Klimaszewski[36], S. Koliiev[52], A. Kondybayeva[83], A. Konoplyannikov[41], P. Kopciewicz[34], R. Kopecna[17], P. Koppenburg[32], M. Korolev[40], I. Kostiuk[32,52], O. Kot[52], S. Kotriakhova[21,38], P. Kravchenko[38], L. Kravchuk[39], R.D. Krawczyk[48], M. Kreps[56], F. Kress[61], S. Kretzschmar[14], P. Krokovny[43,v], W. Krupa[34], W. Krzemien[36], W. Kucewicz[35,t], M. Kucharczyk[35], V. Kudryavtsev[43,v], H.S. Kuindersma[32,33], G.J. Kunde[67], T. Kvaratskheliya[41], D. Lacarrere[48], G. Lafferty[62], A. Lai[27], A. Lampis[27], D. Lancierini[50], J.J. Lane[62], R. Lane[54], G. Lanfranchi[23], C. Langenbruch[14], J. Langer[15], O. Lantwin[50], T. Latham[56], F. Lazzari[29,q], R. Le Gac[10], S.H. Lee[86], R. Lefèvre[9], A. Leflat[40], S. Legotin[83], O. Leroy[10], T. Lesiak[35], B. Leverington[17], H. Li[72], L. Li[63], P. Li[17], S. Li[7], Y. Li[4], Y. Li[4], Z. Li[68], X. Liang[68], T. Lin[61], R. Lindner[48], V. Lisovskyi[15], R. Litvinov[27], G. Liu[72], H. Liu[6], S. Liu[4], A. Loi[27], J. Lomba Castro[46], I. Longstaff[59], J.H. Lopes[2], G.H. Lovell[55], Y. Lu[4], D. Lucchesi[28,l], S. Luchuk[39], M. Lucio Martinez[32], V. Lukashenko[32], Y. Luo[3], A. Lupato[62], E. Luppi[21,f], O. Lupton[56], A. Lusiani[29,m], X. Lyu[6], L. Ma[4], R. Ma[6], S. Maccolini[20,d], F. Machefert[11], F. Maciuc[37], V. Macko[49], P. Mackowiak[15], S. Maddrell-Mander[54], O. Madejczyk[34], L.R. Madhan Mohan[54], O. Maev[38], A. Maevskiy[82], D. Maisuzenko[38], M.W. Majewski[34], J.J. Malczewski[35], S. Malde[63], B. Malecki[48], A. Malinin[81], T. Maltsev[43,v], H. Malygina[17], G. Manca[27,e], G. Mancinelli[10], D. Manuzzi[20,d], D. Marangotto[25,i], J. Maratas[9,s], J.F. Marchand[8], U. Marconi[20], S. Mariani[22,g], C. Marin Benito[48], M. Marinangeli[49], J. Marks[17], A.M. Marshall[54], P.J. Marshall[60], G. Martellotti[30], L. Martinazzoli[48,j], M. Martinelli[26,j], D. Martinez Santos[46], F. Martinez Vidal[47], A. Massafferri[1], M. Materok[14], R. Matev[48], A. Mathad[50], Z. Mathe[48], V. Matiunin[41], C. Matteuzzi[26], K.R. Mattioli[86], A. Mauri[32], E. Maurice[12], J. Mauricio[45], M. Mazurek[48], M. McCann[61], L. Mcconnell[18], T.H. Mcgrath[62], A. McNab[62], R. McNulty[18], J.V. Mead[60], B. Meadows[65], G. Meier[15], N. Meinert[76], D. Melnychuk[36], S. Meloni[26,j], M. Merk[32,80], A. Merli[25], L. Meyer Garcia[2], M. Mikhasenko[48], D.A. Milanes[74], E. Millard[56], M. Milovanovic[48], M.-N. Minard[8], A. Minotti[21], L. Minzoni[21,f], S.E. Mitchell[58], B. Mitreska[62], D.S. Mitzel[48], A. Mödden [15], R.A. Mohammed[63], R.D. Moise[61],

T. Mombächer[46], I.A. Monroy[74], S. Monteil[9], M. Morandin[28], G. Morello[23], M.J. Morello[29,m], J. Moron[34], A.B. Morris[75], A.G. Morris[56], R. Mountain[68], H. Mu[3], F. Muheim[58,48], M. Mulder[48], D. Müller[48], K. Müller[50], C.H. Murphy[63], D. Murray[62], P. Muzzetto[27,48], P. Naik[54], T. Nakada[49], R. Nandakumar[57], T. Nanut[49], I. Nasteva[2], M. Needham[58], I. Neri[21], N. Neri[25,i], S. Neubert[75], N. Neufeld[48], R. Newcombe[61], T.D. Nguyen[49], C. Nguyen-Mau[49,x], E.M. Niel[11], S. Nieswand[14], N. Nikitin[40], N.S. Nolte[64], C. Normand[8], C. Nunez[86], A. Oblakowska-Mucha[34], V. Obraztsov[44], D.P. O'Hanlon[54], R. Oldeman[27,e], M.E. Olivares[68], C.J.G. Onderwater[79], R.H. O'neil[58], A. Ossowska[35], J.M. Otalora Goicochea[2], T. Ovsiannikova[41], P. Owen[50], A. Oyanguren[47], B. Pagare[56], P.R. Pais[48], T. Pajero[63], A. Palano[19], M. Palutan[23], Y. Pan[62], G. Panshin[84], A. Papanestis[57], M. Pappagallo[19,c], L.L. Pappalardo[21,f], C. Pappenheimer[65], W. Parker[66], C. Parkes[62], C.J. Parkinson[46], B. Passalacqua[21], G. Passaleva[22], A. Pastore[19], M. Patel[61], C. Patrignani[20,d], C.J. Pawley[80], A. Pearce[48], A. Pellegrino[32], M. Pepe Altarelli[48], S. Perazzini[20], D. Pereima[41], P. Perret[9], M. Petric[59,48], K. Petridis[54], A. Petrolini[24,h], A. Petrov[81], S. Petrucci[58], M. Petruzzo[25], T.T.H. Pham[68], A. Philippov[42], L. Pica[29,m], M. Piccini[78], B. Pietrzyk[8], G. Pietrzyk[49], M. Pili[63], D. Pinci[30], F. Pisani[48], Resmi P.K[10], V. Placinta[37], J. Plews[53], M. Plo Casasus[46], F. Polci[13], M. Poli Lener[23], M. Poliakova[68], A. Poluektov[10], N. Polukhina[83,u], I. Polyakov[68], E. Polycarpo[2], G.J. Pomery[54], S. Ponce[48], D. Popov[6,48], S. Popov[42], S. Poslavskii[44], K. Prasanth[35], L. Promberger[48], C. Prouve[46], V. Pugatch[52], H. Pullen[63], G. Punzi[29,n], H. Qi[3], W. Qian[6], J. Qin[6], N. Qin[3], R. Quagliani[13], B. Quintana[8], N.V. Raab[18], R.I. Rabadan Trejo[10], B. Rachwal[34], J.H. Rademacker[54], M. Rama[29], M. Ramos Pernas[56], M.S. Rangel[2], F. Ratnikov[42,82], G. Raven[33], M. Reboud[8], F. Redi[49], F. Reiss[62], C. Remon Alepuz[47], Z. Ren[3], V. Renaudin[63], R. Ribatti[29], S. Ricciardi[57], K. Rinnert[60], P. Robbe[11], G. Robertson[58], A.B. Rodrigues[49], E. Rodrigues[60], J.A. Rodriguez Lopez[74], E. Rodriguez Rodriguez[46], A. Rollings[63], P. Roloff[48], V. Romanovskiy[44], M. Romero Lamas[46], A. Romero Vidal[46], J.D. Roth[86], M. Rotondo[23], M.S. Rudolph[68], T. Ruf[48], J. Ruiz Vidal[47], A. Ryzhikov[82], J. Ryzka[34], J.J. Saborido Silva[46], N. Sagidova[38], N. Sahoo[56], B. Saitta[27,e], M. Salomoni[48], D. Sanchez Gonzalo[45], C. Sanchez Gras[32], R. Santacesaria[30], C. Santamarina Rios[46], M. Santimaria[23], E. Santovetti[31,p], D. Saranin[83], G. Sarpis[59], M. Sarpis[75], A. Sarti[30], C. Satriano[30,o], A. Satta[31], M. Saur[15], D. Savrina[41,40], H. Sazak[9], L.G. Scantlebury Smead[63], A. Scarabotto[13], S. Schael[14], M. Schiller[59], H. Schindler[48], M. Schmelling[16], B. Schmidt[48], O. Schneider[49], A. Schopper[48], M. Schubiger[32], S. Schulte[49], M.H. Schune[11], R. Schwemmer[48], B. Sciascia[23], S. Sellam[46], A. Semennikov[41], M. Senghi Soares[33], A. Sergi[24], N. Serra[50], L. Sestini[28], A. Seuthe[15], P. Seyfert[48], Y. Shang[5], D.M. Shangase[86], M. Shapkin[44], I. Shchemerov[83], L. Shchutska[49], T. Shears[60], L. Shekhtman[43,v], Z. Shen[5], V. Shevchenko[81], E.B. Shields[26,j], E. Shmanin[83], J.D. Shupperd[68], B.G. Siddi[21], R. Silva Coutinho[50], G. Simi[28], S. Simone[19,c], N. Skidmore[62], T. Skwarnicki[68], M.W. Slater[53], I. Slazyk[21,f], J.C. Smallwood[63], J.G. Smeaton[55], A. Smetkina[41], E. Smith[50], M. Smith[61], A. Snoch[32], M. Soares[20], L. Soares Lavra[9], M.D. Sokoloff[65], F.J.P. Soler[59], A. Solovev[38], I. Solovyev[38], F.L. Souza De Almeida[2], B. Souza De Paula[2], B. Spaan[15], E. Spadaro Norella[25,i], P. Spradlin[59], F. Stagni[48], M. Stahl[65], S. Stahl[48], P. Stefko[49], O. Steinkamp[50,83], O. Stenyakin[44], H. Stevens[15], S. Stone[68], M.E. Stramaglia[49], M. Straticiuc[37], D. Strekalina[83], F. Suljik[63], J. Sun[27], L. Sun[73], Y. Sun[66], P. Svihra[62], P.N. Swallow[53], K. Swientek[34], A. Szabelski[36], T. Szumlak[34], M. Szymanski[48], S. Taneja[62], A.R. Tanner[54], A. Terentev[83], F. Teubert[48], E. Thomas[48], D.J.D. Thompson[53], K.A. Thomson[60], V. Tisserand[9], S. T'Jampens[8], M. Tobin[4], L. Tomassetti[21,f], D. Torres Machado[1], D.Y. Tou[13], M.T. Tran[49], E. Trifonova[83], C. Trippl[49], G. Tuci[29,n], A. Tully[49], N. Tuning[32,48], A. Ukleja[36], D.J. Unverzagt[17], E. Ursov[83], A. Usachov[32], A. Ustyuzhanin[42,82], U. Uwer[17], A. Vagner[84], V. Vagnoni[20], A. Valassi[48], G. Valenti[20], N. Valls Canudas[85], M. van Beuzekom[32], M. Van Dijk[49], E. van Herwijnen[83], C.B. Van Hulse[18], M. van Veghel[79], R. Vazquez Gomez[46], P. Vazquez Regueiro[46], C. Vázquez Sierra[48], S. Vecchi[21],

J.J. Velthuis[54], M. Veltri[22,r], A. Venkateswaran[68], M. Veronesi[32], M. Vesterinen[56], D. Vieira[65], M. Vieites Diaz[49], H. Viemann[76], X. Vilasis-Cardona[85], E. Vilella Figueras[60], A. Villa[20], P. Vincent[13], D. Vom Bruch[10], A. Vorobyev[38], V. Vorobyev[43,v], N. Voropaev[38], K. Vos[80], R. Waldi[17], J. Walsh[29], C. Wang[17], J. Wang[5], J. Wang[4], J. Wang[3], J. Wang[73], M. Wang[3], R. Wang[54], Y. Wang[7], Z. Wang[50], Z. Wang[3], H.M. Wark[60], N.K. Watson[53], S.G. Weber[13], D. Websdale[61], C. Weisser[64], B.D.C. Westhenry[54], D.J. White[62], M. Whitehead[54], D. Wiedner[15], G. Wilkinson[63], M. Wilkinson[68], I. Williams[55], M. Williams[64], M.R.J. Williams[58], F.F. Wilson[57], W. Wislicki[36], M. Witek[35], L. Witola[17], G. Wormser[11], S.A. Wotton[55], H. Wu[68], K. Wyllie[48], Z. Xiang[6], D. Xiao[7], Y. Xie[7], A. Xu[5], J. Xu[6], L. Xu[3], M. Xu[7], Q. Xu[6], Z. Xu[5], Z. Xu[6], D. Yang[3], S. Yang[6], Y. Yang[6], Z. Yang[3], Z. Yang[66], Y. Yao[68], L.E. Yeomans[60], H. Yin[7], J. Yu[71], X. Yuan[68], O. Yushchenko[44], E. Zaffaroni[49], M. Zavertyaev[16,u], M. Zdybal[35], O. Zenaiev[48], M. Zeng[3], D. Zhang[7], L. Zhang[3], S. Zhang[5], Y. Zhang[5], Y. Zhang[63], A. Zharkova[83], A. Zhelezov[17], Y. Zheng[6], X. Zhou[6], Y. Zhou[6], X. Zhu[3], Z. Zhu[6], V. Zhukov[14,40], J.B. Zonneveld[58], Q. Zou[4], S. Zucchelli[20,d], D. Zuliani[28], G. Zunica[62].

[1] *Centro Brasileiro de Pesquisas Físicas (CBPF), Rio de Janeiro, Brazil*
[2] *Universidade Federal do Rio de Janeiro (UFRJ), Rio de Janeiro, Brazil*
[3] *Center for High Energy Physics, Tsinghua University, Beijing, China*
[4] *Institute Of High Energy Physics (IHEP), Beijing, China*
[5] *School of Physics State Key Laboratory of Nuclear Physics and Technology, Peking University, Beijing, China*
[6] *University of Chinese Academy of Sciences, Beijing, China*
[7] *Institute of Particle Physics, Central China Normal University, Wuhan, Hubei, China*
[8] *Univ. Savoie Mont Blanc, CNRS, IN2P3-LAPP, Annecy, France*
[9] *Université Clermont Auvergne, CNRS/IN2P3, LPC, Clermont-Ferrand, France*
[10] *Aix Marseille Univ, CNRS/IN2P3, CPPM, Marseille, France*
[11] *Université Paris-Saclay, CNRS/IN2P3, IJCLab, Orsay, France*
[12] *Laboratoire Leprince-Ringuet, CNRS/IN2P3, Ecole Polytechnique, Institut Polytechnique de Paris, Palaiseau, France*
[13] *LPNHE, Sorbonne Université, Paris Diderot Sorbonne Paris Cité, CNRS/IN2P3, Paris, France*
[14] *I. Physikalisches Institut, RWTH Aachen University, Aachen, Germany*
[15] *Fakultät Physik, Technische Universität Dortmund, Dortmund, Germany*
[16] *Max-Planck-Institut für Kernphysik (MPIK), Heidelberg, Germany*
[17] *Physikalisches Institut, Ruprecht-Karls-Universität Heidelberg, Heidelberg, Germany*
[18] *School of Physics, University College Dublin, Dublin, Ireland*
[19] *INFN Sezione di Bari, Bari, Italy*
[20] *INFN Sezione di Bologna, Bologna, Italy*
[21] *INFN Sezione di Ferrara, Ferrara, Italy*
[22] *INFN Sezione di Firenze, Firenze, Italy*
[23] *INFN Laboratori Nazionali di Frascati, Frascati, Italy*
[24] *INFN Sezione di Genova, Genova, Italy*
[25] *INFN Sezione di Milano, Milano, Italy*
[26] *INFN Sezione di Milano-Bicocca, Milano, Italy*
[27] *INFN Sezione di Cagliari, Monserrato, Italy*
[28] *Universita degli Studi di Padova, Universita e INFN, Padova, Padova, Italy*
[29] *INFN Sezione di Pisa, Pisa, Italy*
[30] *INFN Sezione di Roma La Sapienza, Roma, Italy*
[31] *INFN Sezione di Roma Tor Vergata, Roma, Italy*
[32] *Nikhef National Institute for Subatomic Physics, Amsterdam, Netherlands*
[33] *Nikhef National Institute for Subatomic Physics and VU University Amsterdam, Amsterdam, Netherlands*
[34] *AGH - University of Science and Technology, Faculty of Physics and Applied Computer Science, Kraków, Poland*
[35] *Henryk Niewodniczanski Institute of Nuclear Physics Polish Academy of Sciences, Kraków, Poland*
[36] *National Center for Nuclear Research (NCBJ), Warsaw, Poland*

[37] *Horia Hulubei National Institute of Physics and Nuclear Engineering, Bucharest-Magurele, Romania*
[38] *Petersburg Nuclear Physics Institute NRC Kurchatov Institute (PNPI NRC KI), Gatchina, Russia*
[39] *Institute for Nuclear Research of the Russian Academy of Sciences (INR RAS), Moscow, Russia*
[40] *Institute of Nuclear Physics, Moscow State University (SINP MSU), Moscow, Russia*
[41] *Institute of Theoretical and Experimental Physics NRC Kurchatov Institute (ITEP NRC KI), Moscow, Russia*
[42] *Yandex School of Data Analysis, Moscow, Russia*
[43] *Budker Institute of Nuclear Physics (SB RAS), Novosibirsk, Russia*
[44] *Institute for High Energy Physics NRC Kurchatov Institute (IHEP NRC KI), Protvino, Russia, Protvino, Russia*
[45] *ICCUB, Universitat de Barcelona, Barcelona, Spain*
[46] *Instituto Galego de Física de Altas Enerxías (IGFAE), Universidade de Santiago de Compostela, Santiago de Compostela, Spain*
[47] *Instituto de Fisica Corpuscular, Centro Mixto Universidad de Valencia - CSIC, Valencia, Spain*
[48] *European Organization for Nuclear Research (CERN), Geneva, Switzerland*
[49] *Institute of Physics, Ecole Polytechnique Fédérale de Lausanne (EPFL), Lausanne, Switzerland*
[50] *Physik-Institut, Universität Zürich, Zürich, Switzerland*
[51] *NSC Kharkiv Institute of Physics and Technology (NSC KIPT), Kharkiv, Ukraine*
[52] *Institute for Nuclear Research of the National Academy of Sciences (KINR), Kyiv, Ukraine*
[53] *University of Birmingham, Birmingham, United Kingdom*
[54] *H.H. Wills Physics Laboratory, University of Bristol, Bristol, United Kingdom*
[55] *Cavendish Laboratory, University of Cambridge, Cambridge, United Kingdom*
[56] *Department of Physics, University of Warwick, Coventry, United Kingdom*
[57] *STFC Rutherford Appleton Laboratory, Didcot, United Kingdom*
[58] *School of Physics and Astronomy, University of Edinburgh, Edinburgh, United Kingdom*
[59] *School of Physics and Astronomy, University of Glasgow, Glasgow, United Kingdom*
[60] *Oliver Lodge Laboratory, University of Liverpool, Liverpool, United Kingdom*
[61] *Imperial College London, London, United Kingdom*
[62] *Department of Physics and Astronomy, University of Manchester, Manchester, United Kingdom*
[63] *Department of Physics, University of Oxford, Oxford, United Kingdom*
[64] *Massachusetts Institute of Technology, Cambridge, MA, United States*
[65] *University of Cincinnati, Cincinnati, OH, United States*
[66] *University of Maryland, College Park, MD, United States*
[67] *Los Alamos National Laboratory (LANL), Los Alamos, United States*
[68] *Syracuse University, Syracuse, NY, United States*
[69] *School of Physics and Astronomy, Monash University, Melbourne, Australia, associated to* [56]
[70] *Pontifícia Universidade Católica do Rio de Janeiro (PUC-Rio), Rio de Janeiro, Brazil, associated to* [2]
[71] *Physics and Micro Electronic College, Hunan University, Changsha City, China, associated to* [7]
[72] *Guangdong Provencial Key Laboratory of Nuclear Science, Institute of Quantum Matter, South China Normal University, Guangzhou, China, associated to* [3]
[73] *School of Physics and Technology, Wuhan University, Wuhan, China, associated to* [3]
[74] *Departamento de Fisica , Universidad Nacional de Colombia, Bogota, Colombia, associated to* [13]
[75] *Universität Bonn - Helmholtz-Institut für Strahlen und Kernphysik, Bonn, Germany, associated to* [17]
[76] *Institut für Physik, Universität Rostock, Rostock, Germany, associated to* [17]
[77] *Eotvos Lorand University, Budapest, Hungary, associated to* [48]
[78] *INFN Sezione di Perugia, Perugia, Italy, associated to* [21]
[79] *Van Swinderen Institute, University of Groningen, Groningen, Netherlands, associated to* [32]
[80] *Universiteit Maastricht, Maastricht, Netherlands, associated to* [32]
[81] *National Research Centre Kurchatov Institute, Moscow, Russia, associated to* [41]
[82] *National Research University Higher School of Economics, Moscow, Russia, associated to* [42]
[83] *National University of Science and Technology "MISIS", Moscow, Russia, associated to* [41]
[84] *National Research Tomsk Polytechnic University, Tomsk, Russia, associated to* [41]
[85] *DS4DS, La Salle, Universitat Ramon Llull, Barcelona, Spain, associated to* [45]
[86] *University of Michigan, Ann Arbor, United States, associated to* [68]

[a] *Universidade Federal do Triângulo Mineiro (UFTM), Uberaba-MG, Brazil*
[b] *Hangzhou Institute for Advanced Study, UCAS, Hangzhou, China*

[c] *Università di Bari, Bari, Italy*
[d] *Università di Bologna, Bologna, Italy*
[e] *Università di Cagliari, Cagliari, Italy*
[f] *Università di Ferrara, Ferrara, Italy*
[g] *Università di Firenze, Firenze, Italy*
[h] *Università di Genova, Genova, Italy*
[i] *Università degli Studi di Milano, Milano, Italy*
[j] *Università di Milano Bicocca, Milano, Italy*
[k] *Università di Modena e Reggio Emilia, Modena, Italy*
[l] *Università di Padova, Padova, Italy*
[m] *Scuola Normale Superiore, Pisa, Italy*
[n] *Università di Pisa, Pisa, Italy*
[o] *Università della Basilicata, Potenza, Italy*
[p] *Università di Roma Tor Vergata, Roma, Italy*
[q] *Università di Siena, Siena, Italy*
[r] *Università di Urbino, Urbino, Italy*
[s] *MSU - Iligan Institute of Technology (MSU-IIT), Iligan, Philippines*
[t] *AGH - University of Science and Technology, Faculty of Computer Science, Electronics and Telecommunications, Kraków, Poland*
[u] *P.N. Lebedev Physical Institute, Russian Academy of Science (LPI RAS), Moscow, Russia*
[v] *Novosibirsk State University, Novosibirsk, Russia*
[w] *Department of Physics and Astronomy, Uppsala University, Uppsala, Sweden*
[x] *Hanoi University of Science, Hanoi, Vietnam*